

Local spin valve effect in lateral (Ga,Mn)As/GaAs spin Esaki diode devices

M. Ciorga, C. Wolf, A. Einwanger, M. Utz, D. Schuh, and D. Weiss
Experimentelle und Angewandte Physik, University of Regensburg, D-93040 Regensburg, Germany.

(Received 10 February 2011; accepted 18 April 2011; published online 5 May 2011)

We report here on a local spin valve effect observed unambiguously in lateral all-semiconductor all-electrical spin injection devices, employing $p^+-(\text{Ga,Mn})\text{As}/n^+-\text{GaAs}$ Esaki diode structures as spin aligning contacts. We discuss the observed local spin-valve signal as a result of the interplay between spin-transport-related contribution and the tunneling anisotropic magnetoresistance of the magnetic contacts. The magnitude of the spin-related magnetoresistance change is equal to 30Ω which is twice the magnitude of the measured non-local signal. *Copyright 2011 Author(s). This article is distributed under a Creative Commons Attribution 3.0 Unported License. [doi:10.1063/1.3591397]*

There has been recently a big progress on all-electrical spin injection and detection in lateral semiconductor devices with GaAs-based^{1,2} and Si transport channels.³ Most of the reported experiments were performed on devices operating in a *non-local* (NL) configuration, in which spin accumulation, generated in the transport channel, is probed by a detector contact placed within a certain distance from the injector, outside the current path. The electrical signal which is detected in such a configuration is then a measure of a pure spin current flowing beneath a detector.^{4,5} Whereas this technique proved to be powerful at studying problems related to electrical spin injection and detection, it may not be sufficient for employing in operational spintronic devices, e.g. spin FET.⁶ A prerequisite for several concepts of a spin transistor is the electrical spin signal in *local* configuration, i.e., with spin-polarized charge current flowing between spin-polarized source and drain contacts. The measure of a spin signal is then a relative magnetoresistance change $\Delta R/R_P$ where $\Delta R = R_{AP} - R_P$ and $R_{P(AP)}$ is the resistance measured for parallel (antiparallel) configuration of magnetizations in source and drain contacts.

The conditions required for the observation of an efficient electrical spin signal were discussed extensively in some theoretical papers.⁷⁻⁹ According to those studies the crucial parameter governing the efficiency is the contact tunnel resistance R_b^* at the interface between ferromagnetic material and semiconductor, or, speaking more precisely, the ratio of R_b^* and the product $r_N = \rho_N \lambda_N$, where ρ_N, λ_N are the resistivity and spin diffusion length of the non-magnetic semiconducting material, respectively. A high value of the parameter R_b^*/r_N enables efficient spin injection overcoming the so-called *conductivity mismatch*¹⁰ between ferromagnet and non-magnetic material. A too high ratio R_b^*/r_N makes spins relax before they can be detected, preventing this way an efficient electrical detection of the signal. As a result there exists a window for the possible values of the parameter $R \leq R_b^*/r_N$ for which the obtained electrical spin signal is optimal.^{7,8} This window is given by $(W/t_N)(L/\lambda_N)^2 \ll R_b^*/r_N \ll (W/t_N)$, where L and t_N is, respectively, the length and the thickness of the channel and W is the width of the contacts. Outside this window one could still measure the signal but its amplitude decreases, e.g., for values above the upper limit the MR signal is proportional to r_N/R_b^* .⁷ The above mentioned condition applies both to non-local and local measurements, however in the latter the measured spin signal must compete with magnetoresistance effects at the source and drain contacts, making actual detection of the signal difficult. As R_b^*/r_N is usually pretty high for metal/semiconductor interfaces Fert *et al.*⁸ suggested that transport channels



from other than semiconducting materials, e.g carbon nanotubes, could be much more suitable for spin-FET type of devices.

In this paper we report on the local spin valve signal observed in all-semiconductor lateral devices employing $p^+-(\text{Ga,Mn})\text{As}/n^+-\text{GaAs}$ Esaki diode source and drain contacts. An Esaki diode structure in the contacts ensures that under small applied bias electrons can tunnel between the valence band of $(\text{Ga,Mn})\text{As}$ and the conduction band of GaAs .^{11–13} In our previous work^{2,14} we reported on a successful implementation of an efficient all-electrical spin injection and detection scheme in such a system, demonstrated by non-local measurements. We measured a relatively high spin injection efficiency P of $\approx 50\%$ for low bias currents $|I| \leq 10\mu\text{A}$. The value of the ratio $R_b^*/r_n \approx 100$ for those devices was outside of the optimal range, which for that sample was $1 \ll R_b^*/r_n \ll 4$. Nonetheless a local spin valve signal in the range of $\approx 0.1\%$ could be expected.⁸ The fact, that we could not obtain antiparallel configuration of the contacts magnetization² in those devices made however measurements in local configuration very difficult. Here we present measurements on a similar device, however with a slightly different contact geometry. We clearly observe different switching fields for employed source and drain contacts and a clear spin valve signal in a local configuration. The amplitude of the signal being 0.1% is certainly not optimal yet but consistent with the prediction of Ref. 8. We discuss in the end that it should be feasible to optimize the parameter R_b^*/r_n for this type of devices to the optimal value.

The experiments were performed at $T = 3.6\text{K}$ on devices of a similar type as the one used in Ref. 2. The schematic of the device is shown in Fig. 1(a). The sample features six magnetic Esaki diode contacts to the transport channel. Four contacts in the middle (2–5) are used to inject or detect spins in the channel. The size of those contacts is $(4 \times 50 \mu\text{m}^2)$ and the spacing between their centers is $10 \mu\text{m}$ between pairs 3–2, 4–3 and $20 \mu\text{m}$ between the pair 5–4. Two outside contacts (1, 6), placed around $300 \mu\text{m}$ from the center area, are much bigger ($150 \times 150 \mu\text{m}^2$) and are used as reference contacts in non-local measurements. The Esaki diodes consist of 50 nm of $\text{Ga}_{0.95}\text{Mn}_{0.05}\text{As}$ and 8 nm of $n^+-\text{GaAs}$, with $n^+ = 6 \times 10^{18}\text{cm}^{-3}$. The transport channel is a $1\mu\text{m}$ thick $n-\text{GaAs}$ layer with $n = 2.7 \times 10^{16}\text{cm}^{-3}$. Between the diode and the channel a 15 nm thick GaAs transition $n^+ \rightarrow n$ layer is also used. The mesa is oriented along the $[110]$ and contacts along the $[1\bar{1}0]$ direction. In Fig. 1(b) one can see typical results of the non-local spin-valve (NLSV) measurements with spins injected at the contact 2 and an external magnetic field applied along $[1\bar{1}0]$. NLSV signal observed at the detector 3 is shown in the bottom panel whereas in the upper one we show the three-terminal (3T) voltage V_{2-6} , which is a measure of the magnetoresistance of the interface.¹⁴ From the dependence of the amplitude of the NLSV signal on injector–detector separation, shown in (d), we estimate the spin diffusion length in the channel as $8.3\mu\text{m}$. The bias dependence of the product of the resistance and area of the injector contact, which is a measure of R_b^* , is shown in Fig. 1(c). Given the measured resistivity of the channel, $\rho_N = 1.3 \times 10^{-3}\Omega\text{m}$, and the spin diffusion length $\lambda_N = 8.3 \mu\text{m}$ we get $R_b^*/r_n \approx 2 - 400$ for $I = \pm 5 \mu\text{A}$ (the current used in further measurements). The R_b^*/r_n value is then even slightly bigger compared to our previous samples, whereas the boundary values of the optimal range are approximately the same. The switching behavior of the contacts is however different. We get information on the latter from 3T measurements thanks to the tunneling anisotropic magnetoresistance (TAMR) effect¹⁵ at the Esaki diode contacts.¹⁶ One can clearly see in Fig. 1(b) that the switching fields observed in V_{2-6} correspond to the higher switching field value observed in NL signal of V_{3-6} . The lower switching fields we thus attribute to the detector contact 3. Although the exact switching mechanism of the contacts is beyond the scope of this paper, we would like to point to the different orientation of the contacts as a possible reason for the different switching behavior observed in devices investigated in Ref. 2 and current devices. In the former ones the contacts were aligned along $[100]$, i.e., one of the cubic easy axes for $(\text{Ga,Mn})\text{As}$ (the other being $[010]$). In the current devices contacts were aligned along the $[1\bar{1}0]$ direction, i.e., along the cubic hard axis which is at the same time the easy axis of the superimposed uniaxial anisotropy.¹⁷ Additionally, due to the thicker $(\text{Ga,Mn})\text{As}$ layer ($50 \mu\text{m}$ compared to $20 \mu\text{m}$), we could expect bigger effects due to the lithographically-induced shape anisotropy.¹⁸ The small variations in width between different contacts could then lead to the observed small changes of coercive fields of $\approx 2 \text{ mT}$, which allows the observation of a local spin valve signal.

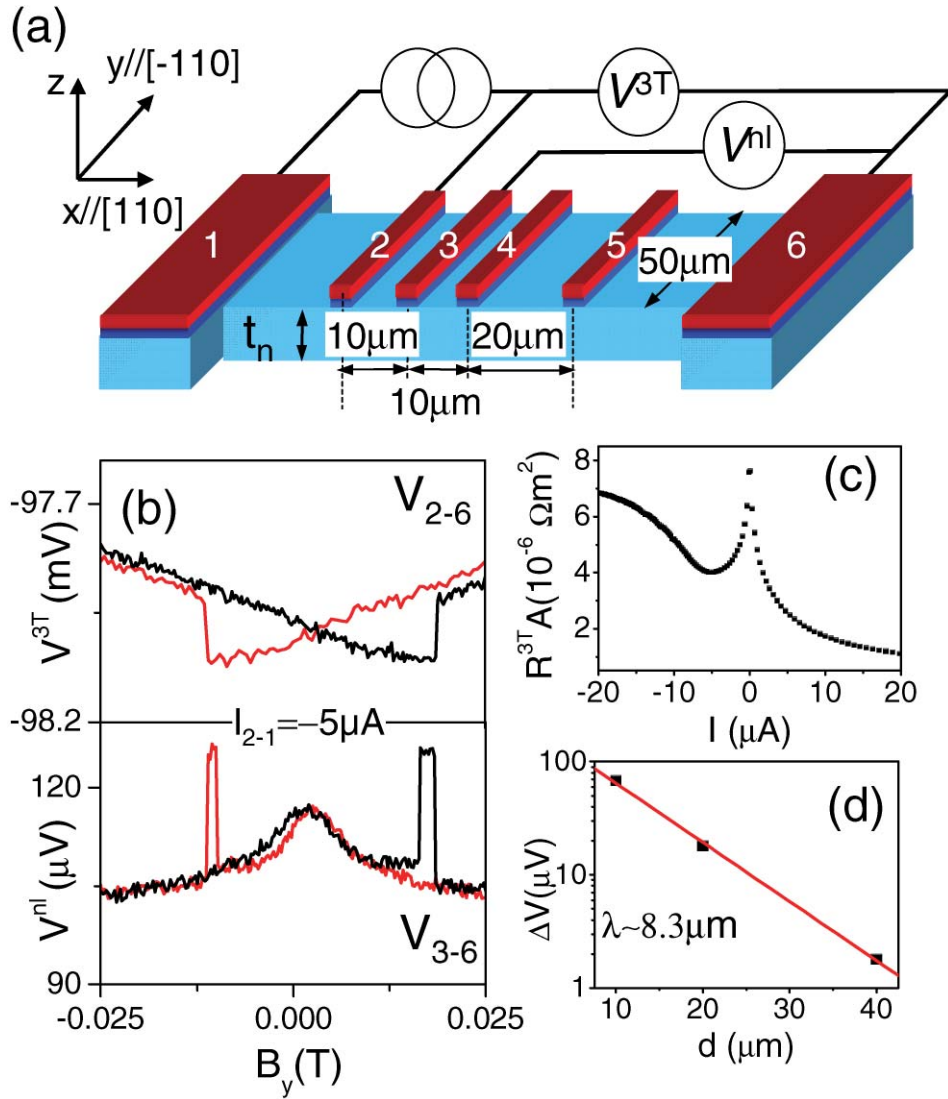


FIG. 1. (a) Schematics of the experimental device; (b) typical dependence of the non-local (NL) voltage (bottom) and three-terminal (3T) voltage (top) on in-plane magnetic field. Measurement configuration as shown in (a); (c) bias dependence of the resistance-area product for contact 2 at $B=0$, typical for all used contacts. (d) dependence of the NLSV signal on injector–detector separation. All measurements were performed at $T=3.6\text{K}$.

The results of local spin valve (LSV) measurements involving contacts 3 and 4, separated by $10\ \mu\text{m}$, are shown in the middle panel of Fig. 2. The resistance in local configuration R^{loc} is the sum of the channel resistance and the resistance of the individual contacts. Any MR effects observed in R^{loc} are then a superposition of effects observed in R^{3T} and the investigated spin transport effects in the channel. We compare then the local measurements with the measurements performed on contact 4 (top panel) and contact 3 (bottom). One can clearly see that the switching fields observed in the MR traces of individual contacts match very well the switching fields observed in LSV measurements. When we subtract the resistance jumps observed in those 3T traces ($36\ \Omega$ and $5\ \Omega$ for contact 4 and 3, respectively) from the resistance jumps observed in LSV signal we obtain the amplitude $\Delta R^{loc} = 30\ \Omega$, which is then the amplitude of the local magnetoresistance change due to magnetization switching in source and drain contacts between parallel and antiparallel configuration. This gives us relative change $\Delta R/R \approx 0.1\%$, which is consistent with the findings of Ref. 8, given the value of R_b^*/r_N in our devices.

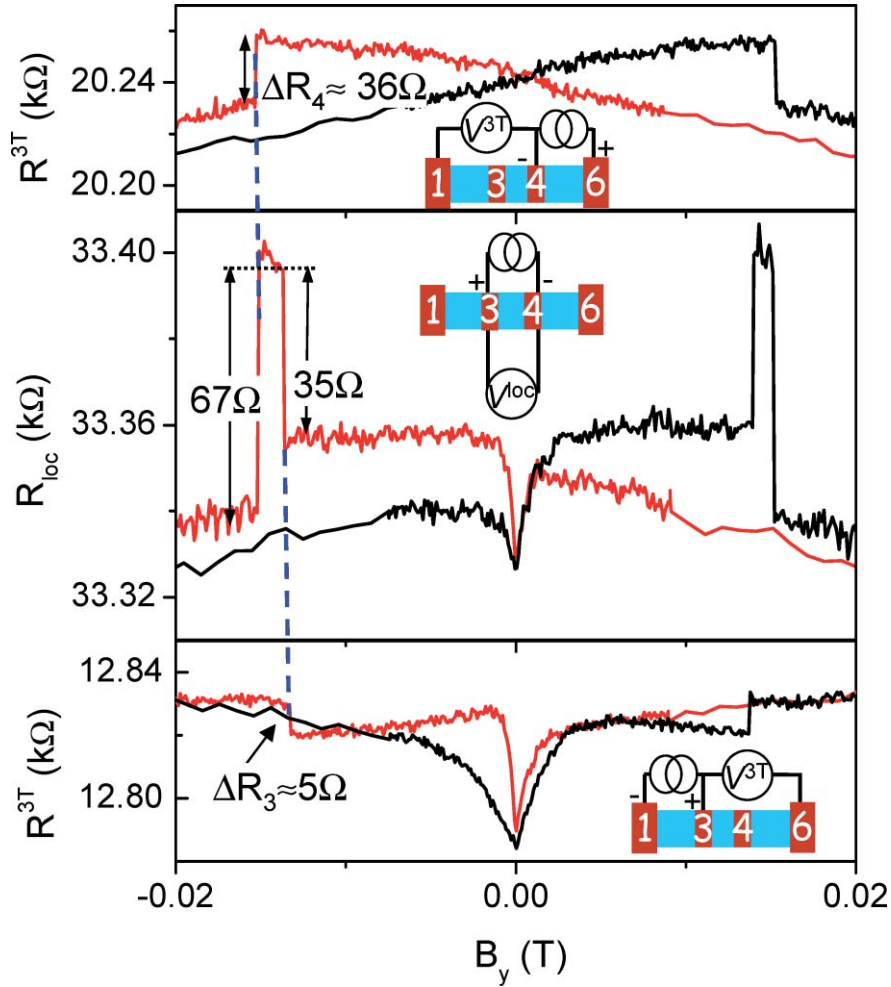


FIG. 2. Local magnetoresistance curve measured between contacts 3 and 4 (middle panel) vs. 3T magnetoresistance curves of the corresponding individual contacts. Measurements performed for the injection current of $\pm 5 \mu A$ at $T=3.6$ K. Measurement configurations are shown as insets.

To check further that the measured ΔR is indeed due to spin-polarized transport we compare LSV and NLSV measurements in Fig. 3. The former is shown in the middle panel. For clarity we show only the results of a down-field sweep in the range around the SV feature. The plotted local data are obtained by subtracting MR traces of individual contacts from the local measurements. As a result we obtain a curve with a clear SV signal with the amplitude $\Delta R = 30 \Omega$, as discussed in the previous paragraph. In the top and the bottom panels we show NL resistance curves measured between contacts 3–1 and 4–6, with the applied currents $I_{4-6} = -5 \mu A$ and $I_{3-1} = 5 \mu A$, respectively. We see that switching field values in the NLSV signal match very well those observed for LSV signal. The amplitude of the NLSV ΔR^{nl} is in both cases around 15Ω , i.e., $\Delta R^{loc} = 2\Delta R^{nl}$. The latter is expected from theory¹⁹ (was also observed in graphene-based devices²⁰), confirming that the spin-valve-like signal observed in the local configuration is indeed due to spin-polarized transport.

Let us now discuss shortly the possibilities of improving some of the device parameters in order to increase the amplitude of the LSV signal. To lower the value of R_b^*/r_N one needs either to lower R_b^* or to increase $r_N = \rho_N \lambda_N$. The latter should be done easily by lowering the doping that would increase both resistivity ρ_N and spin diffusion length λ_N . This is what we did here in comparison to devices investigated in Ref. 2. As a result we increased r_N from $5 \times 10^{-10} \Omega m^2$ to $1 \times 10^{-8} \Omega m^2$. Unfortunately R_b^* increased by roughly the same factor. We would like to point out here, however, that we checked many devices from the same wafer material and some of them showed

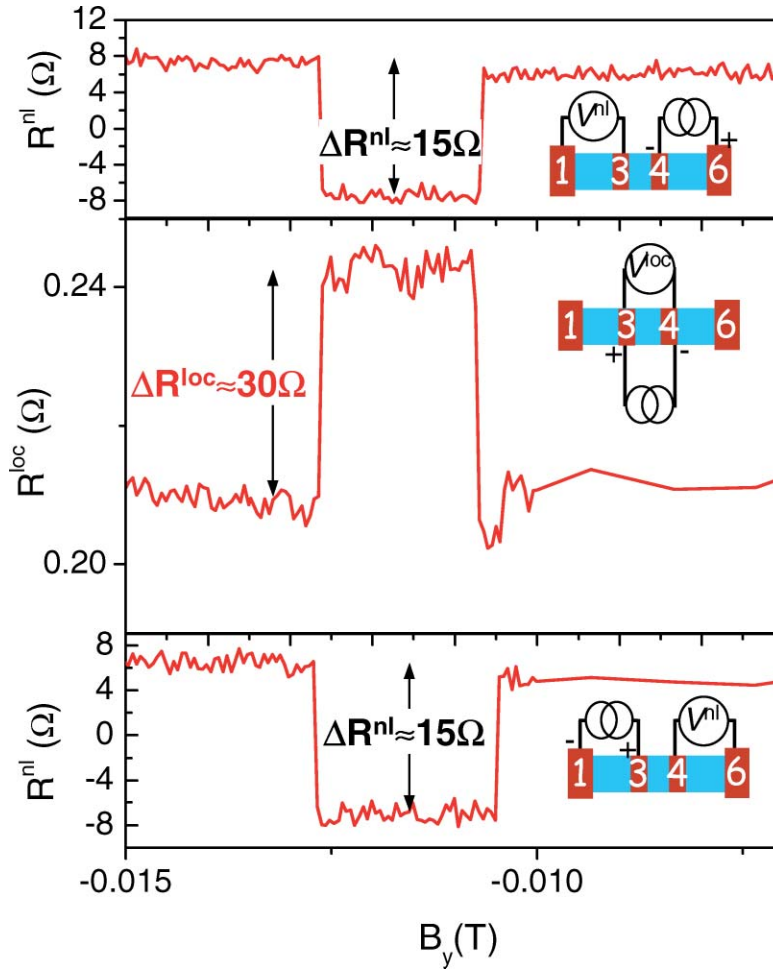


FIG. 3. Local SV signal (middle panel) vs. NLSV signals (top and bottom panels). The LSV curve was obtained by subtracting the 3T resistance of both involved contacts (R_{3T}^{3T} and R_{3T}^{4T}) from the local resistance $R_{3,4}^{loc}$ measured between contacts 3 and 4. Measurements were performed for the injection current of $\pm 5 \mu\text{A}$ at $T=3.6 \text{ K}$. Measurement configurations are shown as insets.

$R_b^* \approx 3 \times 10^{-8} \Omega\text{m}^2$, i.e., values even slightly lower than those investigated in Ref. 2. Similarly as in those other devices we were however not able to obtain an antiparallel configuration of the contacts magnetizations. The different values of R_b^* for different devices suggests either not uniform wafer parameters or that the fabrication process could affect the actual interface resistance. Further work on the subject would require to understand and control those effects to keep R_b^* as low as possible and to bring the values for LSV above 10%. This would be a very reasonable number in terms of application in possible devices.

In summary, we have demonstrated unambiguous observation of a local spin valve effect in lateral all-semiconductor spin injection devices. Although the absolute amplitude of the signal is not very big, our experiments show that optimizing some parameters of our devices, namely the interface resistance, and increasing the amplitude of local spin valve signal is feasible for this type of devices.

This work has been supported by the Deutsche Forschungsgemeinschaft (DFG) through SFB689 project.

¹ X. Lou, C. Adelmann, S. A. Crooker, E. S. Garlid, J. Zhang, K. S. Madhukar Reddy, S. D. Flexner, C. J. Palmström, and P. A. Crowell, *Nature Phys.* 3, **197** (2007).

² M. Ciorga, A. Einwanger, U. Wurstbauer, D. Schuh, W. Wegscheider, and D. Weiss, *Phys. Rev. B* **79**, 165321 (2009).

- ³ S. P. Dash, S. Sharma, R. S. Patel, M. P. de Jong, and R. Jansen, *Nature* **462**, 491 (2009).
- ⁴ M. Johnson and R. H. Silsbee, *Phys. Rev. Lett.* **55**, 1790 (1985).
- ⁵ F. J. Jedema, A. T. Filip, and B. J. van Wees, *Nature* **410**, 345 (2001).
- ⁶ S. Datta and B. Das, *Appl. Phys. Lett.* **56**, 665 (1990).
- ⁷ A. Fert and H. Jaffrès, *Phys. Rev. B* **64**, 184420 (2001).
- ⁸ A. Fert, J. M. George, H. Jaffrès, and R. Mattana, *IEEE Transactions on Electron Devices B* **54**, 21 (2007).
- ⁹ H. Dery, Ł. Cywiński, and L. J. Sham, *Phys. Rev. B* **73**, 041306 (2006).
- ¹⁰ G. Schmidt, D. Ferrand, L. W. Molenkamp, A. T. Filip, and B. J. van Wees, *Phys. Rev. B* **62**, R4790 (2000).
- ¹¹ M. Kohda, Y. Ohno, K. Takamura, F. Matsukura, and H. Ohno, *Jpn. J. Appl. Phys.* **40**, L1274 (2001).
- ¹² E. Johnston-Halperin, D. Lofgreen, R. K. Kawakami, D. K. Young, L. Coldren, A. C. Gossard, and D. D. Awschalom, *Phys. Rev. B* **65**, 041306 (2002).
- ¹³ P. Van Dorpe, Z. Liu, W. Van Roy, V. F. Motsnyi, M. Sawicki, G. Borghs, and J. De Boeck, *Appl. Phys. Lett.* **84**, 3495 (2004).
- ¹⁴ A. Einwanger, M. Ciorga, U. Wurstbauer, D. Schuh, W. Wegscheider, and D. Weiss, *Appl. Phys. Lett.* **95**, 152101 (2009).
- ¹⁵ C. Gould, C. Rüster, T. Jungwirth, E. Girgis, G. M. Schott, R. Giraud, K. Brunner, G. Schmidt, and L. W. Molenkamp, *Phys. Rev. Lett.* **93**, 117203 (2004).
- ¹⁶ M. Ciorga, M. Schlapps, A. Einwanger, S. Geißler, J. Sadowski, W. Wegscheider and D. Weiss, *New J. Phys.* **9**, 351 (2007).
- ¹⁷ M. Sawicki, K.-Y. Wang, K. W. Edmonds, R. P. Campion, C. R. Staddon, N. R. S. Farley, C. T. Foxon, E. Papis, E. Kamińska, A. Piotrowska, T. Dietl, and B. L. Gallagher, *Phys. Rev. B* **71**, 121302 (2005).
- ¹⁸ S. Hünpfner, K. Pappert, J. Wensch, K. Brunner, C. Gould, G. Schmidt, L. W. Molenkamp, M. Sawicki and T. Dietl, *Appl. Phys. Lett.* **90**, 102102 (2007).
- ¹⁹ F. J. Jedema, M. S. Nijboer, A. T. Filip, and B. J. van Wees, *Phys. Rev. B* **67**, 085319 (2003).
- ²⁰ Wei Han, K. Pi, K. M. McCreary, Yan Li, Jared J. I. Wong, A. G. Swartz, and R. K. Kawakami, ArXiv 1008.3209